doi:10.1093/brain/aws056 Brain 2012: 135; 1937–1946 | 1937

BRAIN
A JOURNAL OF NEUROLOGY

Functional immaturity of cortico-basal ganglia networks in Gilles de la Tourette syndrome

Yulia Worbe,[1,2,3,4,5,*] Caroline Malherbe,[6,7,*] Andreas Hartmann,[1,2,3,4,5,8] Mélanie Pélégrini-Issac,[6,7] Arnaud Messé,[6,7] Marie Vidailhet,[1,2,3,4,5] Stéphane Lehéricy[1,2,3,4,5,9] and Habib Benali[6,7]

1 Inserm, Groupe Hospitalier Pitié-Salpêtrière, Assistance Publique–Hôpitaux de Paris, Centre d'Investigation Clinique CIC 9503, Pôle des Maladies du Système Nerveux, Paris, France
2 UPMC Univ Paris 6, UMR-S975, CRICM, Centre de Recherche de l'Institut du Cerveau et de la Moelle épinière, Paris, France
3 Inserm, U975, CRICM, Centre de Recherche de l'Institut du Cerveau et de la Moelle épinière, Paris, France
4 CNRS, UMR 7225, CRICM, Centre de Recherche de l'Institut du Cerveau et de la Moelle épinière, Paris, France
5 ICM–Institut du Cerveau et de la Moelle épinière, Paris, France
6 UPMC Univ Paris 6, UMR-S 678, LIF, Laboratoire d'Imagerie Fonctionnelle, Paris, France
7 Inserm, U678, LIF, Laboratoire d'Imagerie Fonctionnelle, Paris, France
8 Groupe Hospitalier Pitié-Salpêtrière, Assistance Publique-Hôpitaux de Paris, Centre de Référence National Maladie Rare 'Syndrome Gilles de la Tourette', Pôle des Maladies du Système Nerveux, Paris, France
9 Centre de NeuroImagerie de Recherche–CENIR, Paris, France

*These authors contributed equally to this work.

Correspondence to: Yulia Worbe,
Centre de Recherche de l'Institut du Cerveau et de la Moelle épinière (CRICM),
Hôpital Pitié-Salpêtrière,
47–91 boulevard de l'Hôpital,
Paris, F-75013, France
E-mail: yw327@cam.ac.uk

Gilles de la Tourette syndrome is a clinically heterogeneous disorder with poor known pathophysiology. Recent neuropathological and structural neuroimaging data pointed to the dysfunction of cortico-basal ganglia networks. Nonetheless, it is not clear how these structural changes alter the functional activity of the brain and lead to heterogeneous clinical expressions of the syndrome. The objective of this study was to evaluate global integrative state and organization of functional connections of sensori-motor, associative and limbic cortico-basal ganglia networks, which are likely involved in tics and behavioural expressions of Gilles de la Tourette syndrome. We also tested the hypothesis that specific regions and networks contribute to different symptoms. Data were acquired on 59 adult patients and 27 gender- and age-matched controls using a 3T magnetic resonance imaging scanner. Cortico-basal ganglia networks were constructed from 91 regions of interest. Functional connectivity was quantified using global integration and graph theory measures. We found a stronger functional integration (more interactions among anatomical regions) and a global functional disorganization of cortico-basal ganglia networks in patients with Gilles de la Tourette syndrome compared with controls. All networks were characterized by a shorter path length, a higher number of and stronger functional connections among the regions and by a loss of pivotal regions of information transfer (hubs). The functional abnormalities correlated to tic severity in all cortico-basal ganglia networks, namely in premotor, sensori-motor, parietal and cingulate cortices and medial thalamus. Tic complexity was correlated to functional abnormalities in sensori-motor and associative networks, namely in insula and putamen. Severity of obsessive–compulsive disorder was correlated with functional abnormalities in associative and limbic networks, namely in orbito-frontal and prefrontal dorsolateral cortices. The results suggest that the pattern of functional changes in cortico-basal ganglia networks in

Received August 18, 2011. Revised January 4, 2012. Accepted January 5, 2012. Advance Access publication March 19, 2012

patients could reflect a defect in brain maturation. They also support the hypothesis that distinct regions of cortico-basal ganglia networks contribute to the clinical heterogeneity of this syndrome.

Keywords: cortico-basal ganglia networks; graph theory; Gilles de la Tourette syndrome; resting-state functional MRI
Abbreviations: Y-BOCS = Yale-Brown Obsessive-Compulsive Scale; YGTSS = Yale Global Tic Severity Scale

Introduction

Gilles de la Tourette syndrome (GTS) is characterized by the persistence of motor and vocal tics often associated with psychiatric co-morbidity leading to its heterogeneous clinical expression (Cavanna *et al*., 2009).

This heterogeneity of GTS symptoms is suggested to result from the dysfunction of distinct cortico-basal ganglia circuits (Mink, 2003) probably due to aberrant neuronal development of cortex and basal ganglia. Several neuropathological studies in GTS showed both decreased number and deviant distribution of striatal GABA-ergic and achetylcholine interneurons (Kalanithi *et al*., 2005; Kataoka *et al*., 2010) and abnormalities in pallidal projection neurons (Haber *et al*., 1986). These could result both in structural changes and functional abnormalities in cortico-basal ganglia networks in neuroimaging studies.

Indeed, in patients with GTS, previous studies have reported dysfunction of cortico-basal ganglia circuits at different levels. Precisely, cortical structural changes were found in prefrontal, sensori-motor, anterior cingulate, insular, parietal and temporal regions (Peterson *et al*., 2001; Sowell *et al*., 2008; Muller-Vahl *et al*., 2009; Fahim *et al*., 2010). Structural abnormalities were also reported in striatum and globus pallidus (Peterson *et al*., 2003), cerebellum (Makki *et al*., 2008; Tobe *et al*., 2010) and thalamus (Miller *et al*., 2011). Moreover, several studies pointed to spread microstructural abnormalities in white matter in patients with GTS (Neuner *et al*., 2010, 2011).

It has also been suggested by structural neuroimaging studies that functionally segregated sensori-motor, associative and limbic cortico-basal ganglia networks could specifically contribute to clinical expressions (Worbe *et al*., 2010) of GTS comprising simple (Sowell *et al*., 2008; Thomalla *et al*., 2009) and complex tics (Worbe *et al*., 2010) or psychiatric co-morbidities (Bloch *et al*., 2005; Ludolph *et al*., 2008), respectively.

Nonetheless, it remains unclear how previously identified structural abnormalities could influence the pattern of functional connections among anatomical regions and lead to symptom expression. Resting-state functional MRI connectivity measures the synchronization in slow blood oxygen level-dependent signal fluctuations between different brain regions at rest and is a potential tool to answer the aforementioned question (Damoiseaux and Greicius, 2009). The dynamics of this intrinsic activity may reflect some aspects of the functional capacity of neural systems and can consequently be considered appropriate to study brain function in different conditions (Greicius *et al*., 2009). A novel method for analysing resting-state functional MRI data based on graph theory allows characterization of the connections of spontaneous brain functional networks (Bullmore and Sporns, 2009). This theoretical analysis suggests that brain networks are organized according to small-world architecture in which anatomically neighbouring brain regions (nodes) have more connections (edges) with each other than with distant nodes. Such organization is suggested to satisfy the competitive demands of brain networks in local and global information processing (Kaiser and Hilgetag, 2006). In GTS, one study so far has addressed the question of brain functional capacity using resting-state functional MRI (Church *et al*., 2009) and shown decreased maturity of fronto-parietal and cingulo-opercular cortical networks due to abnormal patterns of connections between functional nodes in paediatric patients. In adult patients with GTS, one study has pointed to abnormal functional connections within the amygdala (Werner *et al*., 2010). However, none of these studies explored cortico-basal ganglia networks in GTS using resting-state functional MRI despite a growing body of evidence that points to specific dysfunction of these networks.

In this study, in accordance with the hypothesis that distinct cortico-basal ganglia circuits contribute to the clinical expression of GTS, we evaluated the functional capacity of sensori-motor, associative and limbic cortico-basal ganglia networks in adult patients with GTS compared to controls using resting-state functional MRI. We focused on adult patients with GTS, as they are an interesting population that offers important insights regarding the mechanisms of symptom persistence and maintenance.

We specifically evaluated the global integrative state (Marrelec *et al*., 2008) and organization of functional connections using graph theory (Bullmore and Sporns, 2009) of each network. We also tested the hypothesis that specific functional nodes contribute to severity and complexity of tics and associated obsessive–compulsive disorder.

Materials and methods

Subjects

A total of 64 adult patients with GTS and 27 controls were included in the study. Five patients were excluded from the final data analysis due to insufficient quality of MRI scans.

The 59 included patients and the controls were matched for gender (males/females: 42/17, patients and 15/12, controls; $P = 0.23$, χ^2 test) and age (years, mean ± SD: 29.92 ± 10.90, patients and 29.70 ± 11.35, controls, $P = 0.94$, *t*-test). The study was approved by the local ethics committee and all participants gave written informed consent prior to the study.

Patients were recruited from the French national reference centre for GTS in Paris and examined by a multidisciplinary team. Tic severity was

Table 1 Clinical characteristics of patients with GTS

	All GTS patients	GTS patients with complex tics	GTS patients with associated obsessive-compulsive disorders*
Number of patients	59	23	22
Males/females	42/17	14/9	19/3
Age (years)	29.92 ± 10.9	30.23 ± 13.29	31.29 ± 8.71
Age of symptom onset (years)	6.69 ± 1.68	7.32 ± 2.17	6.71 ± 1.4
Syndrome duration (years)	23.14 ± 10.48	23.23 ± 12.82	23.82 ± 8.71
YGTSS/50	17.08 ± 6.82	20.91 ± 6.60	15.88 ± 1.15
Motor score	10.83 ± 3.44	13.09 ± 3.73	10.29 ± 1.86
Vocal score	6.42 ± 4.74	8.27 ± 4.89	5.59 ± 4.43
Complexity score	2.12 ± 2.06	3.73 ± 1.93	1.88 ± 1.62
Y-BOCS/40	4.17 ± 6.05	1.76 ± 0.82	12.76 ± 5.89
Medication (% of patients)			
Neuroleptics	38.98	52.17	35.29
Benzodiazepines	8.40	4.35	11.76
Antidepressants	11.86	8.70	23.52
Unmedicated	32.86	30.43	41.17

*Three GTS patients with complex tics also had associated obsessive-compulsive disorders.

assessed using the Yale Global Tic Severity Scale (YGTSS) (Leckman *et al*., 1989). The severity of associated obsessive–compulsive disorder was evaluated by the Yale-Brown Obsessive–Compulsive Scale (Y-BOCS) (Goodman *et al*., 1989). Further clinical details are given in Table 1.

For patients, inclusion criteria were age >18 years and confirmed DSM-IV criteria for GTS (2000). Exclusion criteria were: (i) co-occurring psychopathology established by the M.I.N.I. (Mini International Neuropsychiatric Interview—French version) (Sheehan *et al*., 1998), current depression, substance abuse excluding tobacco, current or previous history of psychosis; and (ii) contraindications to MRI examination.

Controls' inclusion criteria were: age >18 years and no history of neurological or psychiatric disorders. The exclusion criteria were the same as for patients plus previous history of tics (childhood tics) and any type of medication, excluding contraceptive pills for females.

Image acquisition

Data were acquired using a 3T Siemens Trio TIM MRI scanner with body coil excitation and a 12-channel receive phased-array head coil.

Anatomical scans were acquired using sagittal 3D T_1-weighted magnetization-prepared rapid acquisition gradient echo sequences (field of view: 256 mm; repetition time/echo time/inversion time: 2300 ms/ 4.18 ms/ 900 ms; flip angle: 9°; partial Fourier 7/8; one average; voxel size: $1 \times 1 \times 1\,mm^3$).

Functional MRI data of the whole brain were acquired using an echo-planar imaging sequence (field of view: 192 mm; echo time/repetition time: 30 ms/2400 ms; flip angle: 90°; 200 volumes in one session). Each volume consisted of 45 contiguous axial slices (voxel size: $3 \times 3 \times 3\,mm^3$, no gap).

The resting state scans were acquired in one 10-min session. During the scans the subjects were instructed to lie with their eyes closed, think of nothing in particular, and not fall asleep (Damoiseaux *et al*., 2006). At the end of the scan the sleepiness was verified by the self-report.

Image preprocessing

Functional MRI data were preprocessed using the SPM 5 software (http://www.fil.ion.ucl.ac.uk/spm/software/spm5), including slice-timing, motion correction, spatial smoothing with an isotropic Gaussian kernel (full-width at half-maximum 5 mm) and low-pass signal filtering with a cut-off frequency of 0.1 Hz.

To assess the amplitude of movements compared to healthy controls, we computed for each subject the variance of *z*-scored realignment parameters using the SPM 5 software. The mean estimated rotation parameter value was (mean ± SD): for controls 0.016 ± 0.010° (range 0.004–0.077°) and for patients with GTS ($n = 53$) 0.024 ± 0.023° (range 0.004–0.090°) ($P = 0.07$, two-sample *t*-test). The mean estimated translation parameter value was (mean ± SD): for controls: 0.849 ± 0.56 mm (range 0.26–3.0 mm) and for patients with GTS: 1.061 ± 0.70 mm (range 0.23–3.0 mm) ($P = 0.17$, two-sample *t*-test). In six patients we observed excessive movements during scanning with (mean ± SD) rotation 0.08 ± 0.017° and translation 6.5 ± 1.5 mm. We performed the analysis both on reduced ($n = 53$) and whole group ($n = 59$) of patients with GTS and did not find any significant difference in the final results.

Cortical and basal ganglia regions were extracted using spatial independent component analysis as described in the Supplementary material. A combined affine and non-linear T-transformation was calculated between each individual anatomical volume and the Montreal Neurological Institute template, after co-registering all functional MRI volumes on the subject's anatomical image.

The mean time series were calculated across all voxels within each region of interest in the individual space, for each subject.

To ensure that variance due to motion was accounted for in data analysis, the motion parameters, as well as signals from white matter and CSF and linear and quadratic drifts were used as covariates of no interest in a general linear model for the mean time courses in each region considered in the analysis.

Individual correlation matrices (and associated *P*-values) were calculated between all pairs of regions of interest within each functional circuit and subject. The average correlation maps were then

compared between patients with GTS and controls (Supplementary Fig. 1).

The individual correlation matrices were binarized by rejecting all connections with a P-value > 0.05. The obtained individual matrices for each functional network were used in the graph theory analysis.

Selection of regions of interest and construction of brain functional networks

According to an anatomical model (Alexander *et al*., 1986), we defined 91 regions of interest and constructed sensori-motor, associative and limbic networks. The regions of interest were selected from the functional networks obtained by spatial independent component analysis and corresponded to the maxima of connectivity peaks of the group functional networks. All regions of interest were defined as a sphere of 10 voxels in the Montreal Neurological Institute space (voxel size: $3.5 \times 3.5 \times 3.5$ mm).

A total of 61 cortical and 25 basal-ganglia regions of interest were extracted from resting-state functional MRI networks. Each network included the cortical areas and corresponding basal ganglia regions (caudate nucleus, putamen and globus pallidus) as well as corresponding functional parts of the thalamus and cerebellum according to anatomical data obtained from tracking studies in monkeys (Dum and Strick, 2002; Haber and Knutson, 2010) and diffusion tensor imaging in humans (Akkal *et al*., 2007; Habas *et al*., 2009; Kamali *et al*., 2011; O'Muircheartaigh *et al*., 2011).

To complete the limbic network, three pairs of regions of interest that were not present in the resting-state functional MRI networks, namely the medial orbito-frontal cortex, hippocampus and amygdala were added on the basis of the structural literature on GTS (Peterson *et al*., 2007; Haber and Knutson, 2010).

For each network, the anatomical labelling and the MNI coordinates of the region of interest are listed in Supplementary Table 1.

Quantification of functional interactions

Functional connectivity was quantified in three cortico-basal ganglia networks using global integration measure and graph theory.

Global functional integration

Global functional integration quantifies the statistical dependence of the blood oxygen level-dependent signal within functional nodes belonging to a given functional network. A global functional integration close to zero corresponds to regions that behave independently, whereas a high level of global functional integration indicates regions that strongly interact (Marrelec *et al*., 2008). Global functional integration was computed from the covariance matrix of the region of interest mean blood oxygen level-dependent time series (Marrelec *et al*., 2008) as follows:

$$I(Y) = \sum_{i=1}^{N} H(y_i) - H(Y),$$

where $I(Y)$ is the integration of network Y composed of N regions y_i and $H(Y) = \frac{1}{2}\ln\{(2\pi e)^N |\mathrm{cov}(Y)|\}$ is the entropy of Y, with $|.|$ the matrix determinant and *cov* the covariance matrix (Tononi *et al*., 1994).

Graph theory

Graph theory was applied to analyse fine-scale functional properties of each network. Individual graph theory metrics were calculated for each subject using the Brain Connectivity Toolbox (http://www.brain-connectivity-toolbox.net) (Rubinov and Sporns, 2010). Detailed description of metrics computation is given in the Supplementary material.

We first evaluated if networks had small-world properties using the small-worldness coefficient (σ). A network is considered to have small-word properties if $\sigma > 1$. We also calculated the principal hubs, which are the nodes with a maximum number of connections. The hubs facilitate integration between the parts of functional networks and assure network resilience to damage (Rubinov and Sporns, 2010). The hubs were identified using the module z-scores (md): a node is considered as a 'hub' if $md > 1$ (Meunier *et al*., 2010).

The calculated graph theory metrics (Rubinov and Sporns, 2010) were:

– k, the degree, is the number of connections that link a node to the rest of the network.

Nodes with a high k functionally interact with many other nodes in the network. k is an important marker of network development and resilience to damage (Bullmore and Sporns, 2009).

– s, the strength, represents the average weighted connections of the node.
– L, the characteristic path length, is the average shortest path between all pairs of nodes of a network.

L characterizes the ability of the brain to rapidly combine specialized information from distributed regions (functional integration). A shorter L corresponds to a more functionally integrated network.

– C, the clustering coefficient, represents the fraction of the node's neighbours that are also neighbours of each other.
– E_l, the local efficiency, reflects local information transfer among the nodes and represents the robustness of the network to deletion of individual nodes.

The clustering coefficient and the local efficiency both represent the ability of a network to process specialized information within densely interconnected groups of nodes (functional segregation). The higher the clustering co-efficient and local efficiency, the more segregated the network.

Statistical analysis

Comparisons of mean values of global integration and each graph theory measures between patients with GTS and controls were performed using analysis of variance (ANOVA) followed by *ad hoc* comparisons using two-sample t-tests.

Regression between tics severity (YGTSS/50) and graph theory measures was performed using a robust multilinear regression of the responses (measures) on the predictors (clinical score). The data were corrected for multiple comparisons using false discovery rate (FDR) correction.

To identify anatomical regions' contribution to different clinical scores (YTGTSS/50, complexity score of YGTSS and Y-BOCS), we used a step-wise regression analysis to correlate the measures in each region of networks with scores of severity and complexity of YGTSS and Y-BOCS, for each separate graph theory metric. At each step, an F-test was carried out, a region being accepted at $P < 0.05$. To test the stability of the model and selected explanatory variables

we performed bootstrapping of the data (5000 iterations) and obtained the same regions using step-wise regression in each network and in each metric, confirming the stability of the chosen model.

Results

Global functional integration in cortico-basal ganglia networks

The global integration was significantly higher in patients with GTS compared with controls in all networks (mean ± SD): for sensori-motor circuits, 3.33 ± 0.23, patients and 2.25 ± 0.12, controls ($P = 0.003$); for associative circuits, 8.12 ± 0.46, patients and 5.81 ± 0.25, controls ($P = 0.002$); for limbic circuits, 4.14 ± 0.25, patients and 3.27 ± 0.13, controls ($P = 0.023$).

Graph theory measures in cortico-basal ganglia networks

All networks had small-world properties ($\sigma > 1.0$) with the following mean values in patients with GTS compared to controls (mean ± SD, all $P > 0.05$): for sensori-motor circuits, 1.46 ± 0.36, patients and 1.55 ± 0.27, controls; for associative circuits, 1.40 ± 0.19, patients and 1.48 ± 0.12, controls; for limbic circuits, 1.31 ± 0.21, patients and 1.41 ± 0.17, controls.

Using the *md* index, we identified the principal hubs in controls (Fig. 1A): for the sensori-motor network–supplementary motor area and posterior insula bilaterally; ventral premotor cortex and motor part of cerebellum on the left, right primary motor cortex; for the associative network–superior parietal and posterior temporal cortices bilaterally, on the left–prefrontal dorsolateral and ventral anterior part of thalamus, on the right–medial temporal cortex and anterior dorsal putamen; for the limbic network–anterior cingulate cortex bilaterally and left hippocampus. In patients with GTS, no hubs were identified as $md < 1.0$ in all regions of all networks (Fig. 1B).

In graph theory measures comparison, patients with GTS had lower values of L and higher s than controls in all three networks (Fig. 2). In addition, the associative network was characterized by a higher value of E_l and k in patients with GTS compared with controls and limbic networks by a higher value of k. C was not significantly different between patients with GTS and controls in any of the networks (Table 2).

We also compared the group of medicated versus unmedicated and male versus female patients with GTS to control the impact of neuroleptic medication and gender, respectively. We did not find any statistically significant difference whatever the metric studied (all $P > 0.05$) and whatever the network, suggesting neither a medication nor gender effect.

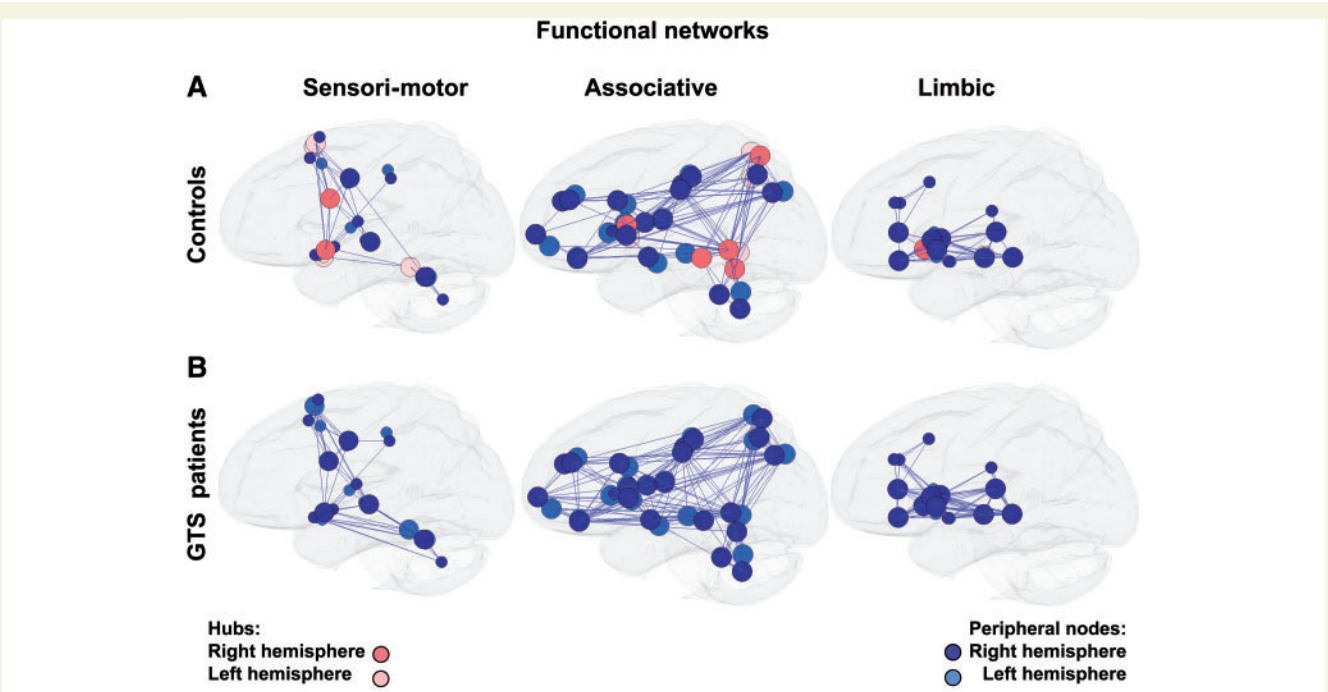

Figure 1 Representation of the functional nodes and the number of connections (k) between the functional nodes in three cortico-basal ganglia networks in controls (**A**) and in patients with GTS (**B**). The purple lines represent connectivity among functional nodes (thresholded at 0.1). The purple circles represent the peripheral functional nodes with size proportional to the value of k (the bigger circles correspond to the higher value of k metric). The hubs in controls are presented as pink circles. No hubs were identified in cortico-basal ganglia networks in patients with GTS.

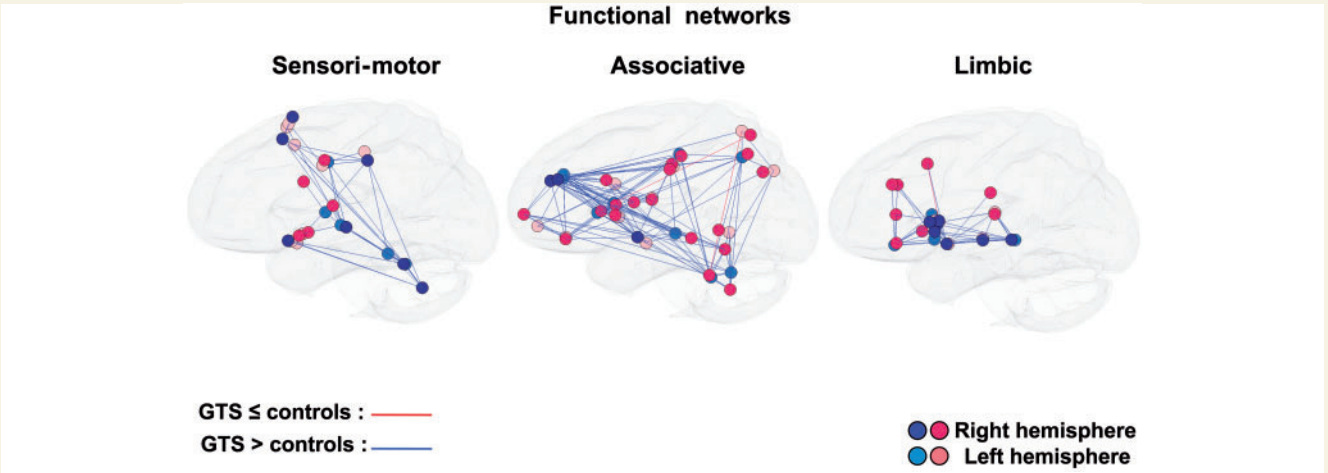

Figure 2 Differences between patients with GTS and controls in strength (*s*) and degree (*k*) of connections among functional nodes in the three cortico-basal ganglia networks. The circles represent the functional nodes of networks. The *s* metric is represented by the colour of the circles. Blue: GTS > controls; pink: GTS = controls. No functional nodes had a superior s value in controls compared to GTS patients. The lines represent the degree of connections (*k*) among the nodes. Blue: GTS > controls; red: GTS ⩽ controls ($P < 0.05$, FDR correction).

Table 2 Graph theory measures values in patients with GTS and controls

	Metric values			YGTSS/50	
Metric	GTS patients	Controls	*P*-value	Correlation	*P*-value
Sensori-motor network:					
k	8.214 ± 3.071	6.704 ± 2.534	**0.030**	**0.3197**	**0.0325**
s	2.067 ± 1.033	1.528 ± 0.711	**0.017**	**0.3458**	**0.0325**
E_l	0.616 ± 0.169	0.542 ± 0.182	0.073	**0.2842**	**0.0363**
C	0.476 ± 0.138	0.424 ± 0.146	0.1	0.2414	0.0650
L	1.757 ± 0.304	1.915 ± 0.315	**0.032**	**−0.2961**	**0.0363**
Associative network:					
k	14.801 ± 5.355	12.236 ± 4.594	**0.026**	**0.3157**	**0.0350**
s	3.627 ± 1.672	2.770 ± 1.287	**0.016**	**0.3329**	**0.0350**
E_l	0.680 ± 0.130	0.618 ± 0.150	**0.043**	0.2304	0.0988
C	0.495 ± 0.125	0.450 ± 0.138	0.1	0.18207	0.1675
L	1.687 ± 0.223	1.810 ± 0.251	**0.018**	**−0.2978**	**0.0367**
Limbic network:					
k	9.772 ± 3.641	7.996 ± 2.425	**0.023**	**0.4227**	**0.0020**
s	2.631 ± 1.422	1.931 ± 0.702	**0.0178**	**0.4378**	**0.0020**
E_l	0.697 ± 0.149	0.651 ± 0.138	0.1	**0.3552**	**0.0057**
C	0.543 ± 0.150	0.499 ± 0.111	0.1	**0.3979**	**0.0025**
L	1.592 ± 0.241	1.727 ± 0.217	**0.015**	**−0.3931**	**0.0025**

Graph theory measures with significant statistical differences in GTS patients compared with controls are in bold. The correlations with severity of tics were performed with total tic score of YGTSS ($P < 0.05$, FDR correction).

Graph theory measures and severity of tics

To link the functional abnormalities of networks to GTS severity, we performed correlations between total tic score of YGTSS (YGTSS/50) and values of graph theory measures (Table 2).

In all networks, YGTSS total tic score positively correlated with values of strength (*s*) and number of connections (*k*) metrics and negatively with value of path length (*L*) metric. A positive correlation of YGTSS total tic score with values of local efficiency of information transfer (E_l) metric was found in sensori-motor and limbic networks.

Functional nodes of cortico-basal ganglia networks contribute to GTS clinical scores

To identify the anatomical regions that contribute to the different clinical scores across the distinct abnormal graph theory metrics, we also performed step-wise regression of each anatomical region of each functional cortico-basal ganglia network with clinical scores (Table 3 and Supplementary Fig. 2).

In sensori-motor networks and in all patients with GTS, tics severity (measured by YGTSS/50 total tic scores) was positively correlated with local efficiency of information transfer (E_l) in the ventral part of left Brodmann area (BA) 6, in the motor part of right cerebellum and negatively with the left primary motor cortex (BA 4). The connection strength (*s*) in the right motor cerebellum also positively correlated with YGTSS/50.

In associative networks and in all GTS patients, tic severity (YGTSS/50) positively correlated with the degree of connections (*k*) and strength of connections (*s*) in the left anterior caudate nucleus and left posterior cingulate (BA 31). The negative correlation of YGTSS/50 with connection strengths (*s*) was found in medio-dorsal parts of the right thalamus, right BA 40 and with degree of connections (*k*) in the left BA 21.

In limbic networks and in all patients with GTS, YGTSS/50 positively correlated with the degree (*k*) of connections in the left BA 32, with strength of connections (*s*) in left anterior pallidum and negatively in medial parts of the thalamus (bilateral).

The presence of complex tics (total complexity score of YGTSS/50 $\geqslant 3$, $n = 23$) was correlated to changes in metrics in sensori-motor and associative networks. Thus, positive correlations were found with degree (*k*) of connections in the posterior cingulate cortex (BA 31) bilaterally and negative, with strength of connections (*s*) in left posterior insular cortex and right parietal cortex (BA 40). The local information transfer (E_l) in the left sensori-motor putamen was also negatively correlated with the complexity score.

In patients with GTS who also presented associated obsessive–compulsive disorder ($n = 22$), the severity of obsessive-compulsive disorders assesed by Y-BOCS was correlated with graph theory measure changes in nodes of associative and limbic networks. We found a positive correlation of total Y-BOCS scores with the degree of connections (*k*) and strength of connections (*s*) in the right medial orbito-frontal cortex and local efficiency of information transfer (E_l) in right prefrontal dorso-lateral cortex (BA 44). A negative correlation with total Y-BOCS scores was found with local efficiency of information transfer (E_l) in the right prefrontal dorso-lateral cortex BA 45.

Table 3 Graph theory measures and functional nodes contribution to the different clinical scores in patients with GTS

Functional nodes	Side	Metric	*P*-value	Correlation
YGTSS/ 50 score: Sensori-motor network				
BA 6	L	E_l	0.0090	positive
BA 4	L	E_l	0.0150	negative
Motor cerebellum	R	E_l	0.0090	positive
	R	s	0.0010	positive
Associative network				
BA 21	L	k	0.0082	negative
BA 31	L	k	0.0018	positive
	L	s	0.0020	positive
BA 40	R	s	0.0400	negative
Anterior caudate	L	k	0.0004	positive
	L	s	0.0005	positive
Thalamus Md	R	s	0.0278	negative
Limbic network				
BA 32	L	k	0.0004	positive
Thalamus ML	Bilateral	s	0.0230	negative
Anterior pallidum	L	s	0.0001	positive
Complexity score of YGTSS: Sensori-motor network				
Posterior insular cortex	L	s	0.0104	negative
Putamen DP	L	E_l	0.0103	negative
Associative network				
BA 31	L	k	0.0469	positive
BA 40	R	s	0.0280	negative
Y-BOCS/ 40 score: Associative network				
BA 44	R	E_l	0.0081	positive
BA 45	R	E_l	0.0008	negative
Limbic network				
Medial OFC	R	k	0.0207	positive
	R	s	0.0148	positive

BA = Brodmann area; L = left hemisphere; Medial OFC = medial part of orbito-frontal cortex; Putamen DP = dorsal part of the posterior putamen; Thalamus Md = mediodorsal thalamic nucleus; Thalamus ML = medial line thalamic nuclei; R = right hemisphere.

Discussion

Using graph theory and resting-state functional MRI data, we showed a stronger global integration and a functional disorganization of cortico-basal ganglia circuits in GTS patients compared with controls. In patients, the networks were characterized by a loss of hubs, a shorter path length, a higher number of and stronger functional connections among the networks. The fine-scale functional disorganization also involved the nodes in each network, which likely contributes to distinct GTS symptoms.

Global integration and intrinsic functional organization of cortico-basal ganglia networks in GTS

Global functional integration and graph theory are complementary methods allowing both the evaluation of global properties and fine region- and connections-related internal organization of functional networks (Marrelec *et al*., 2008; Bullmore and Sporns, 2009).

In patients with GTS, global functional integration was stronger in all cortico-basal ganglia networks, suggesting more functional interactions among anatomical regions. The results obtained from graph theory point to the fact that these functional interactions could result from stronger functional connections and shorter path lengths associated with faster information transfer in the nodes.

In contrast, clustering co-efficient and local efficiency, the measures that reflect the segregation capacity of networks, were not different between patients with GTS and controls, except in associative networks.

Previous studies based on graph theory suggested a concurrent segregation and integration in brain networks during normal brain development (Fair *et al*., 2009) with a progressive weakening of short-range and a strengthening of long-range paths (Fair *et al*., 2009; Power *et al*., 2010). Nonetheless, little is known about the normal functional maturation of cortico-basal ganglia circuits. In one study addressing this question using graph theory (Supekar *et al*., 2009), compared with young adults, children showed a higher number of connections, a lower path length and a higher efficiency of local information transfer between cortical and sub-cortical regions. In contrast, young adults showed stronger cortico-cortical connections mostly between associative and limbic areas.

Consequently, our results suggest that patterns of functional changes in cortico-basal ganglia circuit in GTS could reflect a defect in brain maturation (more and stronger connections between cortex and basal ganglia compared with controls). Accordingly, our data fit well with the developmental theory of GTS suggested by neuropathological studies (Kalanithi *et al*., 2005; Kataoka *et al*., 2010). They are also supported by a recent resting-state functional MRI study in children with GTS (Church *et al*., 2009), which pointed to functional abnormalities of fronto-parietal and cingulo-opercular cortical networks, and diffusion tension imaging on adults with GTS (Neuner *et al*., 2010), which provided evidence for white matter myelination abnormalities, both probably related to brain maturation deficit in GTS.

Role of functional nodes in clinical scores

According to graph theory, the nodes in networks are distinguished as peripheral nodes or as hubs, which are pivotal regions of information transfer (Bullmore and Sporns, 2009). Previous studies using graph theory suggest that hubs are mostly localized within the fronto-parietal and the temporal cortices (Bullmore and Sporns, 2009), within the pallidum in basal ganglia and the thalamus, the hippocampus and the amygdala in sub-cortical structures (Achard *et al*., 2006; Tomasi and Volkow, 2011), which is in line with our data of hub distribution in cortico-basal ganglia networks in controls.

In patients with GTS, the functional reorganization of the networks was characterized by the loss of hubs, with all nodes becoming peripheral. Nonetheless, step-wise regression points to the fact that several functional nodes could play a more important role in distinct clinical symptoms.

The severity and complexity of tics was correlated with abnormal values of graph theory measures in sensori-motor and pre-motor cortices, which is in accordance with dysfunction of sensori-motor pathways found in structural (Peterson *et al*., 2001), functional (Bohlhalter *et al*., 2006) and diffusion tensor (Makki *et al*., 2008) neuroimaging studies in GTS. More severe tics also correlated with more connections in the anterior cingulate cortex. Several functional MRI studies also pointed to the hyperactivity of the anterior cingulate cortex during tic expression (Bohlhalter *et al*., 2006; Kawohl *et al*., 2009). This suggests that pattern of functional connections of anterior cingulate cortex could reflect its elevated functional activity in occurrence of tics. The anterior cingulate cortex has important anatomical connections with the premotor and the supplementary motor cortices (Picard and Strick, 2001) and is suggested to be involved in action control (Paus, 2001). It is also interconnected with the medial thalamic nuclei, which likely regulate its activity (Paus, 2001). In GTS patients, the stronger connections of the medial thalamus correlated with a decreased severity of tics. Consequently, these thalamic nuclei could play a compensatory role in tics via the regulation of the anterior cingulate cortex activity. This is also in line with recent structural data on the thalamus in GTS (Makki *et al*., 2008; Miller *et al*., 2011).

More severe and complex tics also positively correlated with the number of connections of the posterior cingulate cortex. In contrast, the strength of connections in the posterior parietal cortex correlated with a decreased severity of tics. The posterior cingulate cortex is involved in spatial orientation and body topokinesis (Vogt and Laureys, 2005; Vogt *et al*., 2006) and the posterior parietal cortex is involved in movement awareness (Desmurget *et al*., 2009; Desmurget and Sirigu, 2009). Both anatomical regions are strongly interconnected. Thus, it can be suggested that more severe and complex tics possibly result from mismatching of feedback and awareness about the ongoing state of the motor system.

In contrast to tics, the severity of obsessive compulsive disorder was correlated with abnormal graph theory measures in the nodes of the associative and the limbic networks. The strength and number of connections of the medial orbito-frontal cortex were correlated with more severe obsessive–compulsive disorder, which is in line with previous structural (Chamberlain *et al*., 2008) and functional connectivity (Sakai *et al*., 2011) data. The local efficiency of information transfer was correlated with more severe obsessive–compulsive disorder in BA 44 and less severe obsessive compulsive disorder in BA 45, both being a part of the prefrontal dorsolateral cortex. Dysfunction of the dorsolateral prefrontal cortex in patients with obsessive–compulsive disorder has been shown to lead to a lack of a cognitive or an attention flexibility, which maintained the repetitive character of obsessive–compulsive disorder (Menzies *et al*., 2008). Our data therefore suggest that distinct regions of the prefrontal dorsolateral cortex could be involved in both obsessive–compulsive disorder symptom maintenance and compensation, but further investigations on patients with obsessive–compulsive disorder without tics are needed to confirm this hypothesis.

Limitations

A potential bias of this study may be the presence of tic-induced artefacts in the imaging data. Previous studies pointed to the fact that head motion could significantly affect measures of resting-state functional MRI even in healthy young adults (Van Dijk *et al*., 2012) despite compensatory spatial registration

and regression of motion estimated from the data (Power *et al*., 2012).

Although to reduce this potential bias, we asked GTS patients to suppress their tics and subsequently checked for the presence of artefacts, we cannot exclude that some occasional movements might have affected the results. Specifically, the motion bias was shown to produce a reduction in distributed and increases in local functional coupling (Van Dijk *et al*., 2012) that could confound results in GTS patients.

In an effort to regress out movement-induced variance, we included motion realignment parameters as well as physiological signals associated with cardiac and respiratory motion in the general linear model. The variance of the realignment parameters of patients did not significantly differ from that of controls. We also performed the analysis on both the whole and the reduced (i.e. excluding patients with excessive movement) groups of GTS patients and found no significant difference in the results.

Conclusion

In the present study we showed global and fine-scale functional disorganization of cortico-basal ganglia networks in GTS. This functional disorganization could reflect the functional immaturity of cortico-basal ganglia networks, which fits with the developmental hypothesis of GTS. Moreover, our data also support the hypothesis that the dysfunction of cortico-basal ganglia networks and specific anatomical regions could contribute to the clinical heterogeneity of GTS.

Acknowledgements

The authors thank the nurses of the Centre of Clinical Investigation of Pitié-Salpêtrière Hospital and Eric Bardinet, Romain Valabrègue and Kevin Nigaud of the Centre de NeuroImagerie de Recherche for their help in patients' management and scanning.

Funding

This work was supported by a grant from the French National Research Agency (ANR-07-NEURO-023-01).

Supplementary material

Supplementary material is available at *Brain* online.

References

Achard S, Salvador R, Whitcher B, Suckling J, Bullmore E. A resilient, low-frequency, small-world human brain functional network with highly connected association cortical hubs. J Neurosci 2006; 26: 63–72.

Akkal D, Dum RP, Strick PL. Supplementary motor area and presupplementary motor area: targets of basal ganglia and cerebellar output. J Neurosci 2007; 27: 10659–73.

Alexander GE, DeLong MR, Strick PL. Parallel organization of functionally segregated circuits linking basal ganglia and cortex. Annu Rev Neurosci 1986; 9: 357–81.

Bloch MH, Leckman JF, Zhu H, Peterson BS. Caudate volumes in childhood predict symptom severity in adults with GTS. Neurology 2005; 65: 1253–8.

Bohlhalter S, Goldfine A, Matteson S, Garraux G, Hanakawa T, Kansaku K, et al. Neural correlates of tic generation in Gilles de la Tourette syndrome: an event-related functional MRI study. Brain 2006; 129 (Pt 8): 2029–37.

Bullmore E, Sporns O. Complex brain networks: graph theoretical analysis of structural and functional systems. Nat Rev Neurosci 2009; 10: 186–98.

Cavanna AE, Servo S, Monaco F, Robertson MM. The behavioural spectrum of Gilles de la Gilles de la Tourette syndrome. J Neuropsychiatry Clin Neurosci 2009; 21: 13–23.

Chamberlain SR, Menzies L, Hampshire A, Suckling J, Fineberg NA, del Campo N, et al. Orbitofrontal dysfunction in patients with obsessive-compulsive disorder and their unaffected relatives. Science 2008; 321: 421–2.

Church JA, Fair DA, Dosenbach NU, Cohen AL, Miezin FM, Petersen SE, et al. Control networks in paediatric Gilles de la Tourette syndrome show immature and anomalous patterns of functional connectivity. Brain 2009; 132 (Pt 1): 225–38.

Damoiseaux JS, Greicius MD. Greater than the sum of its parts: a review of studies combining structural connectivity and resting-state functional connectivity. Brain Struct Funct 2009; 213: 525–33.

Damoiseaux JS, Rombouts SA, Barkhof F, Scheltens P, Stam CJ, Smith SM, Beckmann CF. Consistent resting-state networks across healthy subjects. Proc Natl Acad Sci U S A 2006; 103: 13848–53.

Desmurget M, Reilly KT, Richard N, Szathmari A, Mottolese C, Sirigu A. Movement intention after parietal cortex stimulation in humans. Science 2009; 324: 811–3.

Desmurget M, Sirigu A. A parietal-premotor network for movement intention and motor awareness. Trends Cogn Sci 2009; 13: 411–9.

Dum RP, Strick PL. Motor areas in the frontal lobe of the primate. Physiol Behav 2002; 77: 677–82.

Fahim C, Yoon U, Das S, Lyttelton O, Chen J, Arnaoutelis R, et al. Somatosensory-motor bodily representation cortical thinning in Tourette: effects of tic severity, age and gender. Cortex 2010; 46: 750–60.

Fair DA, Cohen AL, Power JD, Dosenbach NU, Church JA, Miezin FM, et al. Functional brain networks develop from a "local to distributed" organization. PLoS Comput Biol 2009; 5: e1000381.

Goodman WK, Price LH, Rasmussen SA, Mazure C, Delgado P, Heninger GR, et al. The Yale-Brown obsessive compulsive scale. II. validity. Arch Gen Psychiatry 1989; 46: 1012–6.

Greicius MD, Supekar K, Menon V, Dougherty RF. Resting-state functional connectivity reflects structural connectivity in the default mode network. Cereb Cortex 2009; 19: 72–8.

Habas C, Kamdar N, Nguyen D, Prater K, Beckmann CF, Menon V, et al. Distinct cerebellar contributions to intrinsic connectivity networks. J Neurosci 2009; 29: 8586–94.

Haber SN, Knutson B. The reward circuit: linking primate anatomy and human imaging. Neuropsychopharmacology 2010; 35: 4–26.

Haber SN, Kowall NW, Vonsattel JP, Bird ED, Richardson EP Jr. Gilles de la Tourette's syndrome. A postmortem neuropathological and immunohistochemical study. J Neurol Sci 1986; 75: 225–41.

Kaiser M, Hilgetag CC. Nonoptimal component placement, but short processing paths, due to long-distance projections in neural systems. PLoS Comput Biol 2006; 2: e95.

Kalanithi PS, Zheng W, Kataoka Y, DiFiglia M, Grantz H, Saper CB, et al. Altered parvalbumin-positive neuron distribution in basal ganglia of individuals with Gilles de la Tourette syndrome. Proc Natl Acad Sci USA 2005; 102: 13307–12.

Kamali A, Kramer LA, Hasan KM. Feasibility of prefronto-caudate pathway tractography using high resolution diffusion tensor tractography data at 3T. J Neurosci Methods 2011; 191: 249–54.

Kataoka Y, Kalanithi PS, Grantz H, Schwartz ML, Saper C, Leckman JF, et al. Decreased number of parvalbumin and cholinergic interneurons in the striatum of individuals with Gilles de la Tourette syndrome. J Comp Neurol 2010; 518: 277–91.

Kawohl W, Brühl A, Krowatschek G, Ketteler D, Herwig U. Functional magnetic resonance imaging of tics and tic suppression in Gilles de la Gilles de la Tourette syndrome. World J Biol Psychiatry 2009; 10: 567–70.

Leckman JF, Riddle MA, Hardin MT, Ort SI, Swartz KL, Stevenson J, et al. The Yale Global Tic Severity Scale: initial testing of a clinician-rated scale of tic severity. J Am Acad Child Adolesc Psychiatry 1989; 28: 566–73.

Ludolph AG, Pinkhardt EH, Tebartz van Elst L, Libal G, Ludolph AC, Fegert JM, et al. Are amygdalar volume alterations in children with Gilles de la Tourette syndrome due to ADHD comorbidity? Dev Med Child Neurol 2008; 50: 524–9.

Makki MI, Behen M, Bhatt A, Wilson B, Chugani HT. Microstructural abnormalities of striatum and thalamus in children with Gilles de la Tourette syndrome. Mov Disord 2008; 23: 2349–56.

Marrelec G, Bellec P, Krainik A, Duffau H, Pelegrini-Issac M, Lehericy S, et al. Regions, systems, and the brain: hierarchical measures of functional integration in fMRI. Med Image Anal 2008; 12: 484–96.

Menzies L, Chamberlain SR, Laird AR, Thelen SM, Sahakian BJ, Bullmore ET. Integrating evidence from neuroimaging and neuropsychological studies of obsessive-compulsive disorder: the orbitofronto-striatal model revisited. Neurosci Biobehav Rev 2008; 32: 525–49.

Meunier D, Lambiotte R, Bullmore ET. Modular and hierarchically modular organization of brain networks. Front Neurosci 2010; 4: 200.

Miller AM, Bansal R, Hao X, Sanchez-Pena JP, Sobel LJ, Liu J, et al. Enlargement of thalamic nuclei in Gilles de la Tourette syndrome. Arch Gen Psychiatry 2011 Sep; 67: 955–64.

Mink JW. The Basal Ganglia and involuntary movements: impaired inhibition of competing motor patterns. Arch Neurol 2003; 60: 1365–8.

Muller-Vahl KR, Kaufmann J, Grosskreutz J, Dengler R, Emrich HM, Peschel T. Prefrontal and anterior cingulate cortex abnormalities in Tourette Syndrome: evidence from voxel-based morphometry and magnetization transfer imaging. BMC Neurosci 2009; 10: 47.

Neuner I, Kupriyanova Y, Stocker T, Huang R, Posnansky O, Schneider F, et al. Microstructure assessment of grey matter nuclei in adult tourette patients by diffusion tensor imaging. Neurosci Lett 2011 Jan 3; 487: 22–6.

Neuner I, Kupriyanova Y, Stocker T, Huang R, Posnansky O, Schneider F, et al. White-matter abnormalities in Gilles de la Tourette syndrome extend beyond motor pathways. Neuroimage 2010; 51: 1184–93.

O'Muircheartaigh J, Vollmar C, Traynor C, Barker GJ, Kumari V, Symms MR, et al. Clustering probabilistic tractograms using independent component analysis applied to the thalamus. Neuroimage 2011; 54: 2020–32.

Paus T. Primate anterior cingulate cortex: where motor control, drive and cognition interface. Nat Rev Neurosci 2001; 2: 417–24.

Peterson BS, Choi HA, Hao X, Amat JA, Zhu H, Whiteman R, et al. Morphologic features of the amygdala and hippocampus in children and adults with Gilles de la Tourette syndrome. Arch Gen Psychiatry 2007; 64: 1281–91.

Peterson BS, Staib L, Scahill L, Zhang H, Anderson C, Leckman JF, et al. Regional brain and ventricular volumes in Gilles de la Tourette syndrome. Arch Gen Psychiatry 2001; 58: 427–40.

Peterson BS, Thomas P, Kane MJ, Scahill L, Zhang H, Bronen R, et al. Basal Ganglia volumes in patients with Gilles de la Gilles de la Tourette syndrome. Arch Gen Psychiatry 2003; 60: 415–24.

Picard N, Strick PL. Imaging the premotor areas. Curr Opin Neurobiol 2001; 11: 663–72.

Power JD, Fair DA, Schlaggar BL, Petersen SE. The development of human functional brain networks. Neuron 2010; 67: 735–48.

Power JD, Barnes KA, Snyder AZ, Schlaggar BL, Petersen SE. Spurious but systematic correlations in functional connectivity MRI networks arise from subject motion. Neuroimage 2012; 59: 2142–54.

Rubinov M, Sporns O. Complex network measures of brain connectivity: uses and interpretations. Neuroimage 2010; 52: 1059–69.

Sakai Y, Narumoto J, Nishida S, Nakamae T, Yamada K, Nishimura T, et al. Corticostriatal functional connectivity in non-medicated patients with obsessive-compulsive disorder. Eur Psychiatry 2011; 26: 463–9.

Sheehan DV, Lecrubier Y, Sheehan KH, Amorim P, Janavs J, Weiller E, Hergueta T, Baker R, Dunbar GC. The Mini-International Neuropsychiatric Interview (M.I.N.I.): the development and validation of a structured diagnostic psychiatric interview for DSM-IV and ICD-10. J Clin Psychiatry 1998; 59 (Suppl 20): 22–33; quiz 34–57.

Sowell ER, Kan E, Yoshii J, Thompson PM, Bansal R, Xu D, et al. Thinning of sensori-motor cortices in children with Gilles de la Tourette syndrome. Nat Neurosci 2008; 11: 637–9.

Supekar K, Musen M, Menon V. Development of large-scale functional brain networks in children. PLoS Biol 2009; 7: e1000157.

Thomalla G, Siebner HR, Jonas M, Baumer T, Biermann-Ruben K, Hummel F, et al. Structural changes in the somatosensory system correlate with tic severity in Gilles de la Gilles de la Tourette syndrome. Brain 2009; 132 (Pt 3): 765–77.

Tobe RH, Bansal R, Xu D, Hao X, Liu J, Sanchez J, et al. Cerebellar morphology in Gilles de la Tourette syndrome and obsessive-compulsive disorder. Ann Neurol 2010; 67: 479–87.

Tomasi D, Volkow ND. Association between functional connectivity hubs and brain networks. Cereb Cortex 2011; 21: 2003–13.

Tononi G, Sporns O, Edelman GM. A measure for brain complexity: relating functional segregation and integration in the nervous system. Proc Natl Acad Sci USA 1994; 91: 5033–7.

Van Dijk KR, Sabuncu MR, Buckner RL. The influence of head motion on intrinsic functional connectivity MRI. Neuroimage 2012; 59: 431–8.

Vogt BA, Laureys S. Posterior cingulate, precuneal and retrosplenial cortices: cytology and components of the neural network correlates of consciousness. Prog Brain Res 2005; 150: 205–17.

Vogt BA, Vogt L, Laureys S. Cytology and functionally correlated circuits of human posterior cingulate areas. Neuroimage 2006; 29: 452–66.

Werner CJ, Stocker T, Kellermann T, Wegener HP, Schneider F, Shah NJ, et al. Altered amygdala functional connectivity in adult Tourette's syndrome. Eur Arch Psychiatry Clin Neurosci 2010; 260 (Suppl 2): S95–9.

Worbe Y, Gerardin E, Hartmann A, Valabregue R, Chupin M, Tremblay L, et al. Distinct structural changes underpin clinical phenotypes in patients with Gilles de la Gilles de la Tourette syndrome. Brain 2010; 133 (Pt 12): 3649–60.